The Egyptian Journal of Radiology and Nuclear Medicine (2016) 47, 243–253

Egyptian Society of Radiology and Nuclear Medicine

The Egyptian Journal of Radiology and Nuclear Medicine

www.elsevier.com/locate/ejrnm
www.sciencedirect.com

ORIGINAL ARTICLE

Potential role of quantitative MRI assessment in differentiating high from low-grade gliomas

Eman A.SH. Geneidi [a,*], **Lobna A. Habib** [a], **Nivine A. Chalabi** [a], **Mohamed H. Haschim** [b]

[a] *Ain Shams University, Faculty of Medicine, Radiology Department, Egypt*
[b] *Ain Shams University, Egypt*

Received 25 May 2015; accepted 9 November 2015
Available online 23 December 2015

KEYWORDS

Fractional anisotropy;
Diffusion tensor imaging;
Perfusion weighted imaging;
Glioma;
MRI grading

Abstract *Background:* It is crucial to accurately differentiate HGGs from LGGs, as treatment strategies vary. Our study aims to assess the sensitivity and specificity of fractional anisotropy (FA) values derived from diffusion tensor imaging (DTI) and dynamic contrast enhanced perfusion-weighted imaging (PWI) in differentiating HGGs from LGGs.
Materials: 15 patients with HGGs and 9 LGGs were examined. Mean, Minimal and Maximal FA fractional anisotropy in tumour, necrotic area and in surrounding oedema, as well as (rCBV) ratio of the lesions were measured and compared between LGG and HGG. The efficacy of the above parameters in grading gliomas was evaluated. In perfusion MRI, we measure rCBV ratio as parameter of neovascularity of tumour.
Results: The use of MR DTI had an important role in the grading of brain gliomas as it was accurate in grading 24 cases. There was significant correlation between histopathological grade and FA values measured in tumour and necrotic areas. No positive correlation in perifocal areas could be established. Our results show significant difference between HGG and LGG with mean rCBV ratio as 2.62 & 0.79 with best cut-off value (1.2).
Combined use of MR DTI and MR perfusion added to the accuracy of grading of glioma.

1. Introduction

Imaging plays a crucial role in the management of patients with brain tumours, and the development of new MRI imaging techniques strongly improved the detection and characterization of brain tumours (1).

Advances in imaging, are being used by neurosurgeons to target aggressive areas in gliomas, and to help identify tumour boundaries, functional areas and tracts. Neuro-oncological surgeons need to understand these techniques to help maximize tumour resection, while minimizing morbidity in an attempt to improve the quality of patient outcome. Multimodality MRI is being used for pre-operative imaging assessments and allows informed decisions on operative planning

* Corresponding author.
E-mail address: emangeneidi@hotmail.com (E.A.SH. Geneidi).
Peer review under responsibility of Egyptian Society of Radiology and Nuclear Medicine.

http://dx.doi.org/10.1016/j.ejrnm.2015.11.005

and surgical resection. Each technique has specific advantages over standard imaging (2).

Gliomas are the most common primary tumours of the central nervous system and represent about one third of all intracranial tumours in adults. MRI has been the lifelong established method for evaluating such tumours both before and after treatment. However the use of conventional MRI limits the application of MRI to the morphological information. The newly developed concept of obtaining both morphological and physiological information in a single examination is highly attractive. Roberts et al. study described physiologic imaging as incorporation of many tools. It includes evaluating blood volume, diffusional motions, vascular permeability as well as the cellular metabolic profiles (3).

Hartmann et al. study pointed that despite optimization of sequences and protocols, the classification and grading of gliomas with conventional MR imaging is sometimes unreliable, with the sensitivity for glioma grading ranging from 55.1% to 83.3% (4).

A point of prime importance is that contrast agents in use, are actually non-specific to tumour tissue and their grade, but rather, they enhance in area where the blood-brain barrier has become permeable. Thus we needed to apply a technique that actually assesses tumour neovascularity rather than contrast leakage. This was possible by applying perfusion MR technique (5).

Moreover, the prognosis for patients with gliomas relies on the histopathology grading, whereas the prognosis for those with high-grade gliomas (HGGs) remains very poor compared to the low-grade gliomas (LGGs) (6). In patients with HGGs, surgical resection followed by adjuvant chemo-radiotherapy represents the standard of care (7). As for those with LGGs, the optimal therapeutic measure includes offering extensive resection of the tumour, if possible, and delaying adjuvant radiotherapy postoperatively until the time of glioma progression (8). So, it is crucial to accurately differentiate HGGs from LGGs preoperatively, as well as follow-up on LGG tumours with early detection of any residual/recurrent tumoural regions (see Figs. 1 and 2).

Dynamic susceptibility-weighted contrast-enhanced perfusion-weighted imaging (DSC-PWI) is a well-established technique in grading cerebral gliomas and predicting prognosis (9–13). Law et al. proposed a relative cerebral blood volume (rCBV) ratio cut-off value of 1.75 to distinguish LGG from HGG (11).

As an advanced magnetic resonance images (MRI) technique, diffusion tensor imaging (DTI) provides visibility into the motion of water molecules. Fractional anisotropy (FA) is the commonly used key metric of DTI, which represents a metric of the directionality of molecular movement (14). The value of FA in preoperative grading of gliomas is still controversial.

The purpose of this study is to evaluate various imaging parameters, including maximal rCBV, Mean, Min and Maximal FA that may aid in differentiation of LGG from HGG.

2. Materials and methods

MR examinations of 24 patients (mean age 29 ± 13) were done, 18 male, 6 females with brain tumours. Biopsy of all patients was done and there were 9 patients with LGG and 15 patients with HGG. A standard 1.5 Tesla unit (Gyroscan T10 NT, Philips) with a standard head coil was used. All patients were subjected to the following MRI protocols;

Sequence	Parameters taken
Pre- and postcontrast axial, coronal and sagittal T1 weighted spin echo (T1WI)	(T1 SE) TR of 652 ms, a TE of 13 ms, a 256 × 256 acquisition matrix, a field of view of 240 mm, a slice thickness of 5 mm and a gap of 1 mm
Axial T2 weighted turbo spin echo (T2 WI)	(TR) of 4000 ms, (TE) of 106 m, a slice thickness of 5 mm, a gap of 1 mm, 256 × 256 acquisition matrix, FOV = 240 mm
Axial FLAIR	TR of 9000 ms, a TE of 107 ms, TI 2000 ms a field of view of 240 mm, a slice thickness of 5 mm and a gap of 1 mm
Diffusion Tensor imaging (DTI)	Consisted of a single shot, spin-echo echo planar sequence in 12 encoding directions and a diffusion-weighting factor (*b* value) of 1000 s/mm^2. TR 2800, TE 94, matrix 128 × 128, FOV 240 × 240 mm, number of excitations 2, slice thickness: 2.0/00 and flip angle 90 (degrees)
Perfusion MR	Carried out using a lipid-suppressed echo planar sequence utilizing the following parameters: TR, 1520 s; TE, 32 ms, Slice thickness, 5 mm. axial slice orientation to cover the entire tumour, maximum of 19 slices; Matrix size, 128 × 128; field of view, 240 mm. A series of 40 acquisitions at 1 s interval was acquired. Intravenous contrast injection was done after five baseline acquisitions were acquired. With the pressure injector a dose of 0.2-mmol/kg bodyweight gadopentetate dimeglumine (Gd-DTPA), was injected at a rate of 5 mL/s through an 18-G cannula placed in the antecubital region and immediately followed by 20 ml injection of saline

All the diffusion-weighted images were transferred to the workstation and images were post-processed using the Philips software devised for tractography. The maps obtained were as follows: FA maps, directionally encoded color FA map, 3D fibre tractography maps. The direction and anatomy of the

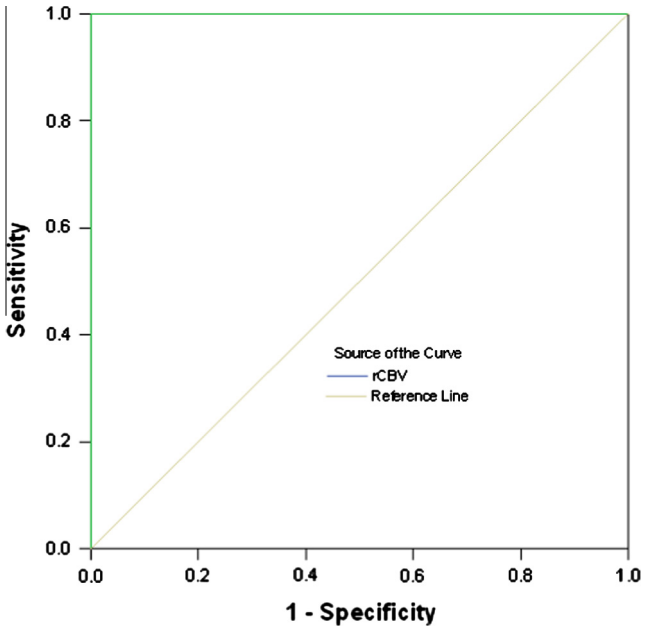

Fig. 1 Diagnostic performance of rCBV ratio parameter in discriminating between HGG & LGG.

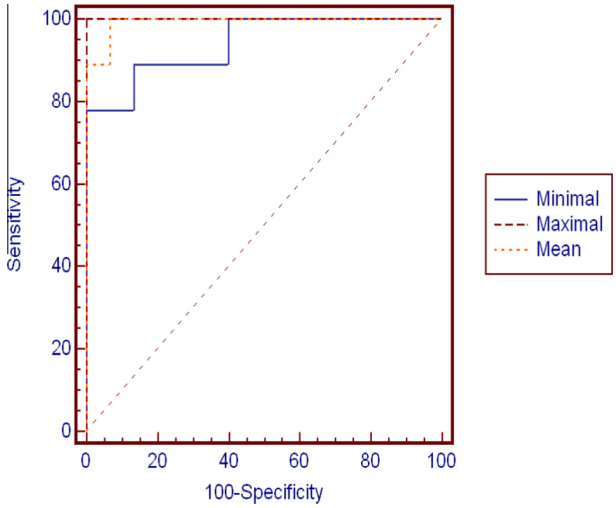

Fig. 2 Bivariate rCBV ratio and (minimal, maximal and mean FA tumour area).

tracts are seen in the directionally-encoded FA maps, where a specific color is assigned to tracts running in the three orthogonal planes. A 3D display of tracts was created. For creating 3D fibre tracts, a ROI (or seed) was drawn (placed) along the course of the tract in the (axial, sagittal or coronal) color encoded FA map in single or consecutive sections. The software then automatically traces the assigned tract and presents it in a 3D manner. Three regions of interest (ROIs) were drawn at tumour solid portion, perifocal area and necrotic area of tumour where FA values are measured. Color-coded DTI maps were analyzed, followed by tractography of individual tracts. In most of patients the tumour was isolated to one hemisphere, The location of each tract and its hue on directional color maps were classified as normal or abnormal, based

Table 1 Descriptive data of the study patients with regard to different parameters.

Parameters	High grade		Low grade	
	Mean	±SD	Mean	±SD
Age (years)	42.33	10.57	16.33	7.71
rCBV ratio	2.62	0.75	0.79	0.20
Tumour FA				
Minimal	137.13	45.33	73.11	23.35
Maximal	293.60	77.83	155.56	25.05
Mean	215.37	60.20	114.33	21.30
Perifocal area FA				
Minimal	296.33	134.22	206.44	101.90
Maximal	473.73	186.05	392.00	238.88
Mean	385.03	155.06	299.22	143.56
Necrotic				
Minimal	29.67	5.76	61.50	26.88
Maximal	80.83	44.09	125.83	41.18
Mean	55.25	22.80	93.67	25.40

Data are expressed as mean ± SD for each parametric.

Table 2 Histopathological grades distribution within study group.

Histopathological	Frequency	Percentages (%)
High grade	15	62.5
Low grade	9	37.5
Total	24	100

Table 3 Comparison between histopathological and (rCBV ratio) of tumour.

	High		Low		*t*-test	
	Mean	±SD	Mean	±SD	*T*	*p*-value
rCBV ratio	2.62	0.74	0.79	0.23	7.157	<0.01 (HS)

Table 4 Diagnostic performance of rCBV ratio in discrimination between HGG & LGG in PWI.

	Cut-off value	Sens.	Spec.	+PV	−PV	AUC
rCBV ratio	>1.2	100.0	100.0	100.0	100.0	100.0

on comparison to the homologous tracts in the contralateral hemisphere, which were unaffected by tumour. We adopted the criteria developed by Cruz et al at 2007 to classify fibre tract involvement into 4 categories: Deviated (Displaced), Oedematous, Infiltrated and Destructed (Disrupted).

For perfusion MRI, series of 40 images was obtained and analyzed, and the start- and end-points of the first pass transit were calculated from the means of the signal intensities of all the pixels covering the brain. Because the change in the $T2^*$ relaxation rate is linearly proportional to the concentration

of contrast in the tissue, the same was calculated on a pixel-to pixel basis using the formula ((S/So)/TE), where So is the baseline signal intensity, S is the change in the signal intensity and TE is the echo time. Thus a time–signal intensity curve was essentially changed to a time–concentration curve.

Analysis was then performed on the time–concentration curve and the various perfusion parameters were calculated. The relative cerebral blood volume (rCBV) maps were generated from an integration of the $\Delta R2^*$ values from the start to the end of the first pass of the contrast. The rCBV of the tumour was normalized with respect to that of the contralateral normal white matter taken as a reference. The CBV and CBF maps were analyzed with respect to heterogeneity on visual inspection and by placing region of interests in hot spots of the tumours. The rCBV ratios were normalized with respect to the contralateral white matter.

Data were analyzed using Statistical Program for Social Science (SPSS) version 18.0. Quantitative data were expressed as mean ± standard deviation (SD). Qualitative data were expressed as frequency and percentage.

The following tests were done:

- Independent-samples *t*-test of significance was used when comparing between two means.
- Chi-square (X^2) test of significance was used in order to compare proportions between two qualitative parameters.
- Pearson's correlation coefficient (*r*) test was used for correlating data.
- Receiver operating characteristic (ROC curve) analysis was used to find out the overall predictivity of parameter in and to find out the best cut-off value with detection of sensitivity and specificity at this cut-off value, positive predictive value (PPV), negative predictive value (NPV) Probability (*P*-value)
  - *P*-value <0.05 was considered significant.
  - *P*-value 0.01 was considered as highly significant.
  - *P*-value >0.05 was considered insignificant.

The placement of ROIs in PWI and DTI data analysis was decided by consensus of 2 of the authors who have 8 and 7 years of experience in MR PWI and DTI data analysis, respectively, who were blinded to the histopathological and clinical information.

3. Results

Twenty-four patients, compromising 18 males and 6 females, ranging in age from 8 to 58 years with a mean age of 29 years were included in the current study. All patients were evaluated with pre- and postcontrast conventional MR studies as well as DTI and contrast enhanced MR perfusion study (Table 1).

We studied 24 patients including 15 cases pathologically proven to have high-grade gliomas, 3 cases didn't enhance on conventional images (20%) while 9 cases proved to have low-grade gliomas, out of which 2 cases showed heterogeneous enhancement (22%).

In perfusion MRI, we measure rCBV ratio as parameter for assessment of neovascularity of tumour in hot spot technique in comparison with the contralateral area, and the results were mean rCBV ratio for HGG & LGG as (2.62 & 0.79 respectively) with cut-off value (1.2).

This table shows the significant difference between histopathological (high and low grades) in regards of rCBV ratio, using independent sample *t*-test, with *p*-value <0.01 HS (see Tables 2–4).

Receiver operating characteristics (ROC) curve was used to define the best cut-off value of the rCBV ratio which was >1.2, with sensitivity of 100, specificity of 100, positive predictive value of 100, negative predictive value of 100 with AUC 100.

In DTI MR examination, we do assessment of tumours by measuring FA values (Min, Max & Mean) at 3 ROIs (at solid

Table 5 Comparison between histopathological and tumour FA of the study group.

Tumour FA (1/1000)	High		Low		*t*-test	
	Mean	±SD	Mean	±SD	*T*	*p*-value
Minimal	137.13	45.33	73.11	23.35	4.631	<0.01 (HS)
Maximal	293.60	77.83	155.56	25.05	5.124	<0.01 (HS)
Mean	215.37	60.20	114.33	21.30	6.82	<0.01 (HS)

Table 6 Diagnostic performance of FA values as a parameter in discrimination between HGG & LGG from tumour portion.

Tumour FA (1/1000)	Cut-off value	Sens.	Spec.	+PV	−PV	AUC
Minimal	>85	93.3	77.8	87.5	87.5	88.9
Maximal	>190	100.0	100.0	100.0	100.0	100.0
Mean	>135	100.0	100.0	100.0	100.0	100.0

Table 7 Comparison between histopathological and perifocal FA of the study group.

Perifocal FA (1/1000)	High		Low		*t*-test	
	Mean	±SD	Mean	±SD	*T*	*p*-value
Minimal	296.33	134.22	206.44	101.90	1.727	0.098
Maximal	473.73	186.05	392.00	238.88	0.937	0.359
Mean	385.03	155.06	299.22	143.56	1.35	0.191

Table 8 Comparison between histopathological grades and necrotic area FA values of the study group.

Necrotic area FA (1/1000)	High		Low		*t*-test	
	Mean	±SD	Mean	±SD	*T*	*p*-value
Minimal	29.67	5.76	61.50	26.88	−4.039	<0.01 (HS)
Maximal	80.83	44.09	125.83	41.18	−2.083	0.054
Mean	55.25	22.80	93.67	25.40	−3.25	<0.01 (HS)

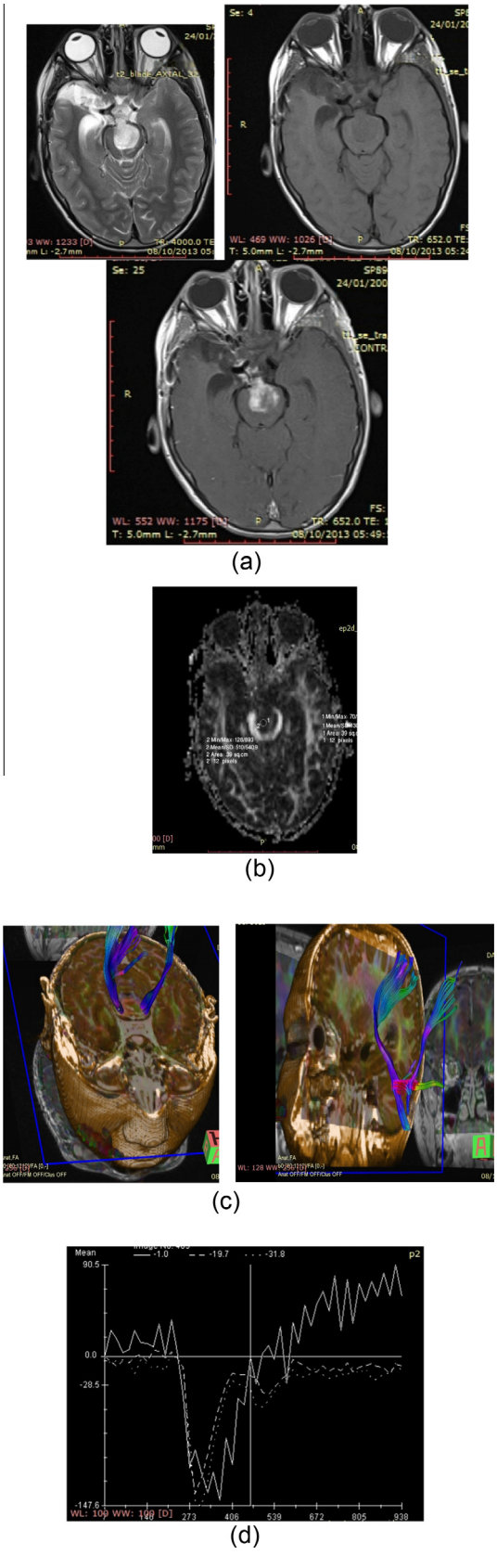

portion of tumour, at perifocal area & necrotic area) for each patient.

First ROI: Solid tumoral portion, FA values were as in following Table 5:

This table shows the significant difference between histopathological (high and low grades) in regard to tumour portion FA values, and there was highly statistically significant difference, using independent sample *t*-test, with *p*-value <0.01 HS.

At tumoural solid portion, ROC curve was used to define the best cut-off value for the Minimal, Maximal and Mean FA, with sensitivity, specificity, positive predictive, negative predictive values and area under the curve (AUC) for each were recorded and compared (see Table 6).

Second ROI: Perifocal area, FA values were as in following Table 7:

This table shows no significant difference among histopathological grades (HGG & LGG) in regard to perifocal FA values, using independent sample *t*-test, with *p*-value >0.05 NS.

The third ROI: Necrotic area of tumour, FA values were as in following Table 8:

This table shows the statistically significant difference between histopathological grades (HGG & LGG) in regard to Min & Mean FA and non-significant Max FA, using independent sample *t*-test.

Combination of perfusion (rCBV ratio) & DTI (FA) MRI examinations with conventional MRI can raise the sensitivity and specificity of performance in grading of gliomas into HGG & LGG upto 100% (see Figs. 3–7).

4. Discussion

The recent advances in brain tumour imaging offer unique anatomical as well as pathophysiological information that provides new insights on brain tumours, directed on facilitating the new therapeutic decisions and proving information regarding the prognosis (15).

Conventional MR imaging readily provides evidence of enhancement, signifying blood-brain barrier breakdown,

Fig. 3 Male patient (8 years old) is complaining from headache for 3 months ago & attacks of vomitting. (a) T2 & T1 (Pre- & Post-contrast) weighted MR imaging show well defined solid mass involving the anterior aspect of midbrain measures $2.3 \times 2 \times 2$ cm in diameter, moderate hypointense T1, hyperintense T2, and heterogenous contrast enhancement in T1 postcontrast. (b) Color coded FA image & quantitative FA image show: Min/Max FA & mean FA values for tumour (1) & perifocal area (2) as marked above in corresponding image. (c) 3D tractography showing smooth lateral displacement of the left corticospinal tracts (d) Susceptibility signal intensity -time curve with regions of interest over tumour (--------) and contralateral brain (. . . . . .) shows low rCBV ratio within the lesion. rCBV = 0.95. *Final MRI diagnosis after DTI and MR perfusion:* low grade glioma displacing tracts rather than infiltrating with low FA values which is further confirmed by low rCBV. *Histopathological report:* Low grade (grade I & II WHO grading).

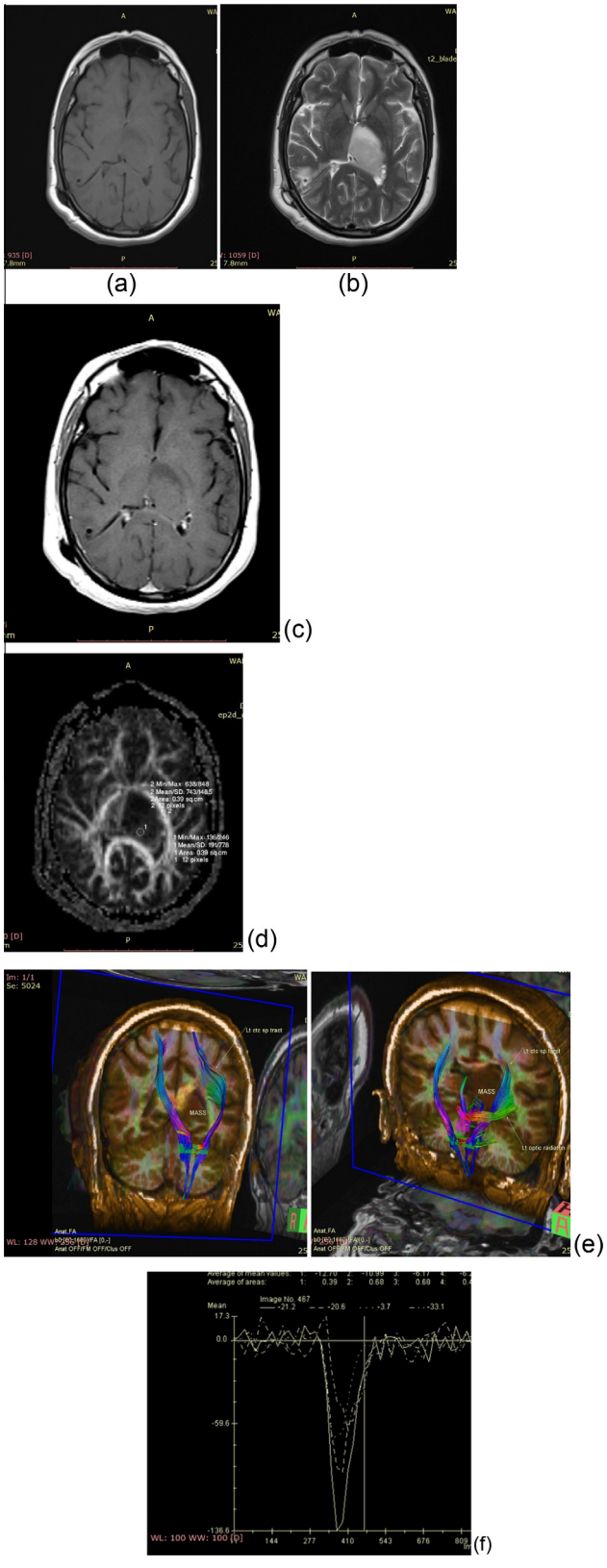

which is often associated with higher tumour grade. However, contrast enhancement alone is not always accurate in predicting tumour grade as encountered in our study.

A study by Law et al., carried out on 160 patients, reported that sensitivity for differentiation between low and high-grade gliomas with conventional MR imaging was 72.5%. (16–18) as characterization depending on contrast enhancement, perifocal oedema, haemorrhage, necrosis and mass effect, can be sometimes difficult esp. in atypical cases. Ginsberg et al. study was performed upon 50 patients, and reported that one fourth of low-grade gliomas (25%) showed enhancement and one fifth of high-grade gliomas (20%) did not (19).

We studied 24 patients including 15 cases pathologically proven to have high-grade gliomas, 3 cases didn't enhance on conventional images (20%) while 9 cases proved to have low-grade gliomas, out of which 2 cases showed heterogeneous enhancement (22%). All patients are examined using conventional MRI pre- and postcontrast, DTI & PWI.

Regarding DTI, three spots (ROIs) were taken in FA map at the following: tumour (solid portion), perifocal area & necrotic area & were considered as parameters to our study. The values of Min, Max and Mean FA in tumour area & the value of Minimal & Mean FA in necrotic area were significantly different in HGG than that in LGG, with higher sensitivity and specificity in the grading of gliomas than the other imaging parameters. Our study could not detect any significant difference between the LGG and HGG with regard to Max, Min & Mean FA in perifocal area & Max FA in necrotic area.

Our results are in consensus with the study by Lee et al. (20) who stated that FA has been used to grade gliomas, and show a trend towards higher FA values in HGG relative to LGG.

Min, Mean and Maximal FA values at tumour areas in our study were also significantly higher in HGG when compared with LGG. These findings are consistent with the results in

Fig. 4 (a–c) T2 & T1 (Pre- & Post-contrast) weighted MR imaging shows the following: well defined soft tissue mass involving the left thalamus and extending downward to involve the central and dorsal aspects of the upper midbrain. It measures around 4.5 * 4.5 * 2.5 cm. It appears as homogenous iso-intense in T1, hyperintense in T2, with minimal perifocal oedema with effacement of third ventricle & shows no significant enhancement in T1 postcontrast. (d) Color coded FA image & quantitative FA image show the following: Min/Max FA & Mean FA values for tumour area (1) & perifocal area (2). (e) 3D tractography showing displacement of the left optic radiation inferomedially & ipsilateral meyer"s loop is crossing along the inferior margin of the mass. (f) Susceptibility signal intensity -time curve with regions of interest over tumour (--------) and contralateral brain area (. . . . . .) shows high rCBV within the lesion. rCBV = 1.8. *Final MRI diagnosis after DTI and MR perfusion:* high-grade glioma displacing tracts with homogenous iso-intense signal in T1 with hyperintense signal in T2 and insignificant enhancement postcontrast with increase perfusion which is indicated by significantly high rCBV and rCBF values. *Histopathological report:* High grade (grade III & IV WHO grading).

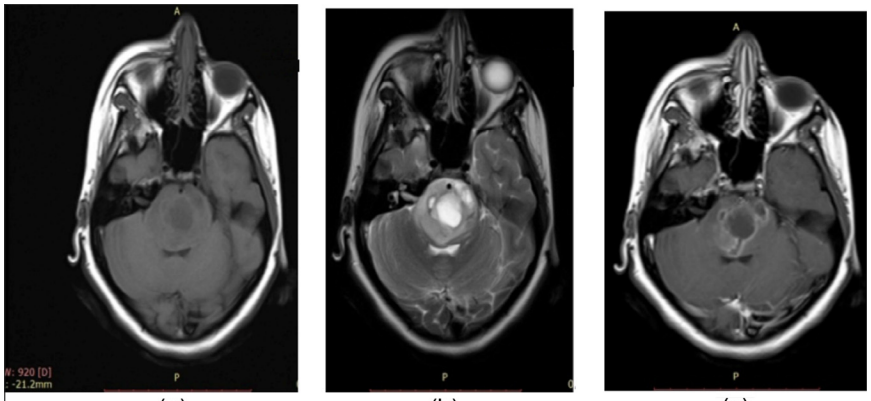

(a) (b) (c)

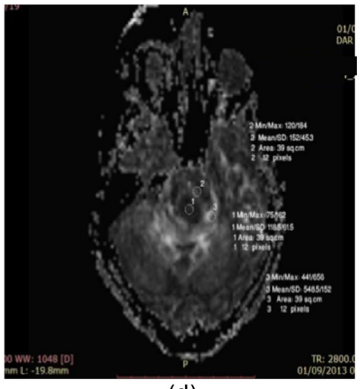

(d)

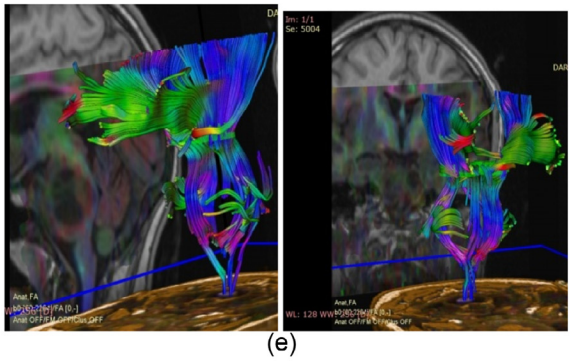

(e)

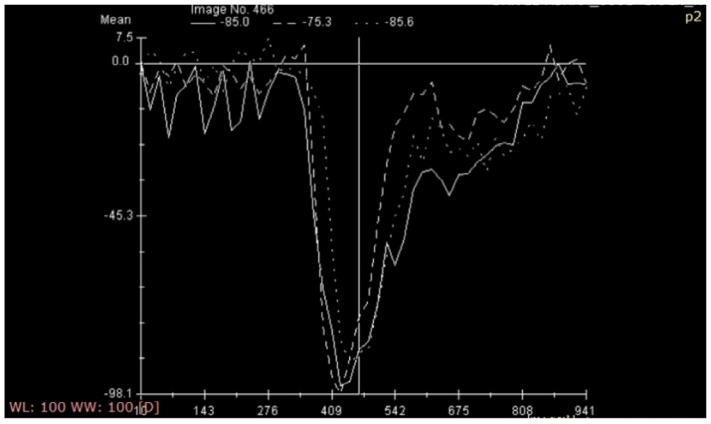
Mean
Image No: 466
-85.0
-75.3
-85.6
p2
7.5
0.0
-45.3
-98.1
WL: 100 WW: 100 [D]
143
276
409
542
675
808
941

(f)

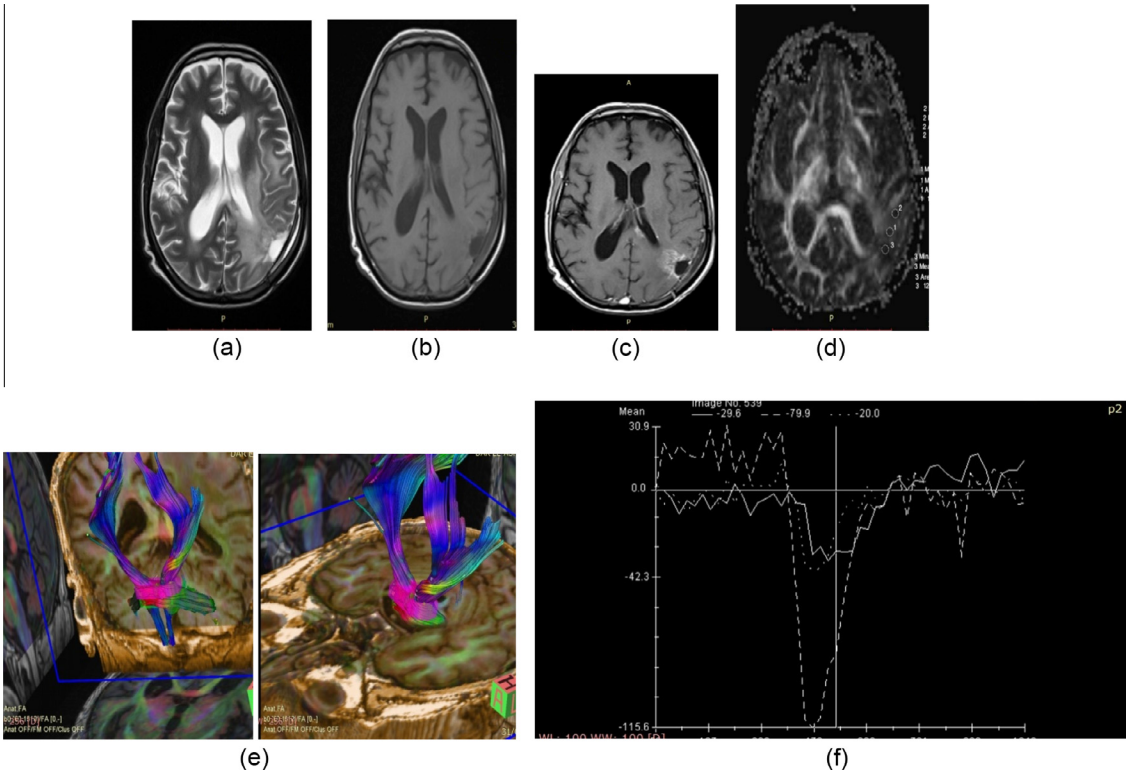

Fig. 6 Male patient (58 y old) complain from convulsions & dysarthria. (a–c) T2 & T1 (Pre- & Post-contrast) weighted MR imaging shows the following: heterogenous mass lesion with area of cystic component and necrosis involving the cortex and subcortical white matter at left temperoparieto-occipital region, appears as hypointense in T1, heterogenous hyperintense in T2, with perifocal oedema & heterogenous enhancement in T1 postcontrast. (d) Color coded FA image & quantitative FA image show: Min/Max FA & mean FA for tumour area (1), perifocal area (2) & necrotic area (3) as marked above in corresponding image. (e) 3D tractography showing displacement of the left optic radiation inferomedially & ipsilateral meyer"s loop is crossing along the inferior margin of the mass. (f) Susceptibility signal intensity -time curve with regions of interest over tumour (--------) and contralateral brain area (. . .. .) shows high rCBV within the lesion. rCBV = 4.2. *Final MRI diagnosis after DTI and MR perfusion:* high-grade glioma displacing tracts with high FA values & heterogeneous signal and enhancement postcontrast with area of necrosis & increase vascularity which is further confirmed by significantly high rCBV value. *Histopathological report:* High grade (grade III & IV WHO grading).

studies by Inoue et al., 2005; Beppu et al., 2005 and Kinoshita et al., 2008 (21–23).

The mechanisms underlying the higher FA values in HGG are complex but can be attributed to the following factors as hypothesized by various authors: Higher tumour cellularity in HGG may positively correlate with higher FA values (24,25). Increase in the degree of directionality of water diffusion due to decrease in extracellular volume (increased cellularity) may also induce increased FA values (25). The pseudo palisading structure in glioblastomas may contribute to the higher FA values similar to the high FA values in meningioma (26).

Our preliminary study not only demonstrate the role of Min, Max & Mean FA in grading of gliomas, but also provided the FA color map, which could easily visualize the tumour content with high FA value. This might be useful in guiding stereotactic biopsy of gliomas, which could easily visualize the tumour content with high FA value. FA Color maps

Fig. 5 Female (12 y old) complaining headache, & weakness in her extremities. (a–c) T2 & T1 (Pre- & Post-contrast) weighted MR imaging shows heterogenous mass lesion with both cystic and solid components noted within pons, hypointense T1, hyperintense T2, and heterogenous contrast enhancement in T1 postcontrast. (d) Color coded FA image & quantitative FA image show the following: Min/Max FA & mean FA values for tumour (2) & perifocal area (3) & necrotic area (1) as marked above in corresponding image. (e) 3D tractography showing compression of corticospinal tracts & displaced anteriorly & laterally by the lesion with sparsed fibres (f) Susceptibility signal intensity -time curve with regions of interest over tumour (--------) and contralateral brain area (. . .. .) shows low rCBV within the lesion. rCBV = 0.9. *Final MRI diagnosis after DTI and MR perfusion:* low-grade glioma displacing tracts rather than infiltrating with low FA values, which is further confirmed by low rCBV. *Pathology report:* Low grade (grade I & II WHO grading).

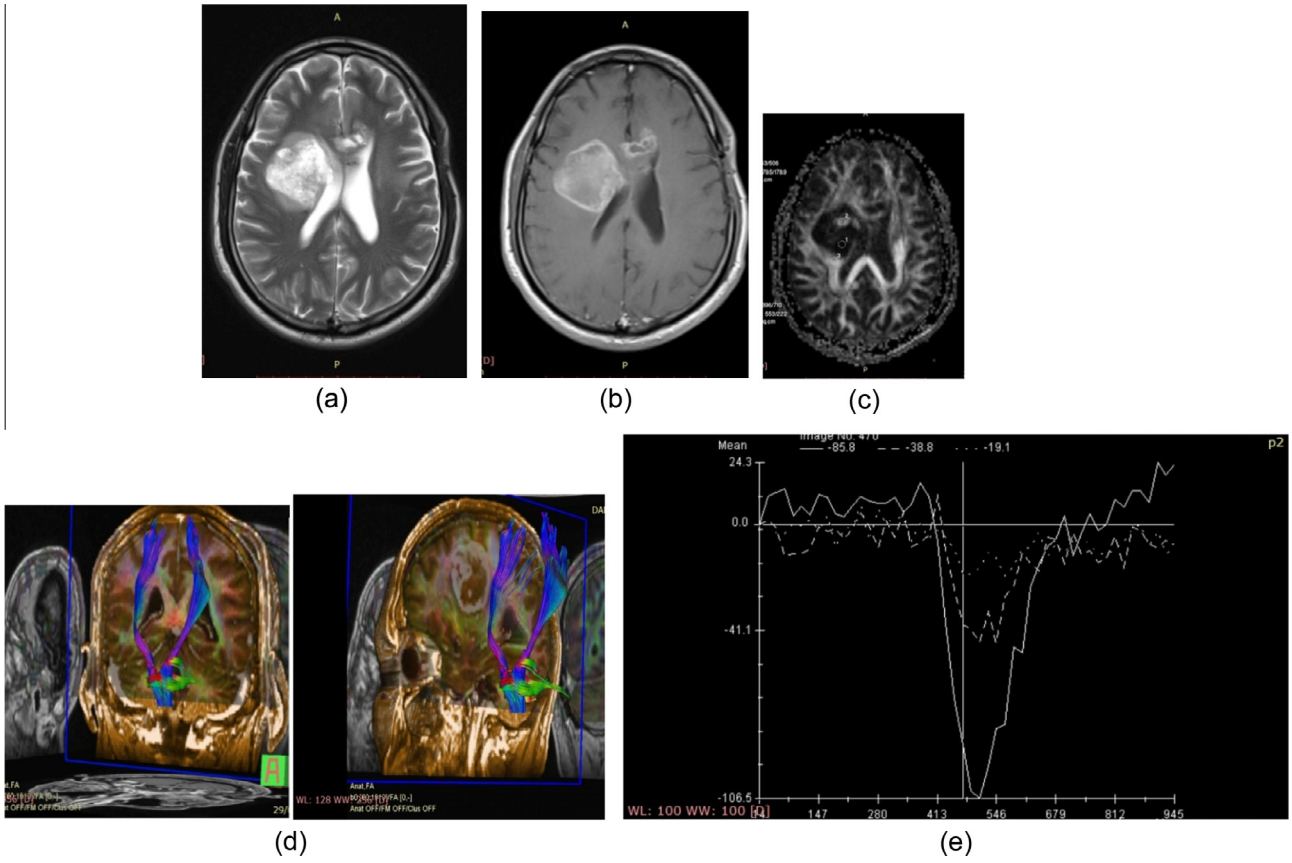

Fig. 7 Male (35 y old) patient present with severe interactable headache, vomitting. (a) & (b) T2 & T1 (Post-contrast) weighted MR imaging shows large heterogenous mass lesion epicentred on right fronto-parietal region 5 × 4.5 cm, extending to the contralateral side with invasion of corpus callosum with positive mass effect. Exhibiting hyperintense T2, and heterogenous enhancement in T1 postcontrast. (c) Color coded FA image & quantitative FA image show the following: Min/Max FA & mean FA for tumour (2) & perifocal area (3) & necrotic area (1) as marked above in corresponding image. (d) 3D tractography showing destruction and infiltration of right corticospinal tract compared to left. (e) Susceptibility signal intensity-time curve with regions of interest over tumour (---------) and contralateral brain (. . . . . .) shows high rCBV ratio within the lesion. rCBV = 2.9. *Final MRI diagnosis after DTI and MR perfusion:* high-grade glioma due to multilocality, crossing midline with necrosis & displacing tracts with high FA values, which is further confirmed by high rCBV. *Pathology report:* high-grade (grade III & IV WHO grading).

in DTI also help in accurate depiction of early recurrent or residual tumour foci for accurate treatment plans.

The sensitivity, specificity & accuracy for FA parameters according to their cut-off values in different areas of the tumour were recorded in our study, yet for any comparison, we need same standards to be scientifically & statistically dependable. There were no clear dependable cut-off values for Min, Max & Mean FA in previous studies to compare with our results, because of differences in samples sizes, ROIs, parameters & the ways parameters were calculated from our study.

The perfusion data of the brain tumours are expressed in terms of rCBV (relative cerebral blood volume), rCBF (relative cerebral blood flow) and MTT (mean transit time), however rCBV is the most important in grading of gliomas followed by rCBF which plays a less important role in tumour differentiation and grading (27).

Wong et al. study reported a significant difference in rCBV between high-grade and low-grade gliomas, with low-grade gliomas often having homogenously low rCBV and high-grade gliomas exhibiting varying degrees of high rCBV. Again no single constant rCBV value could be given for each group (28).

Lev et al. study reported that rCBV for low-grade gliomas is less than 1.5 ± 1.1 and the mean rCBV for high-grade gliomas is about 2.9 ± 1.5 (29). Covarrubias et al.'s study further agreed with Lev et al.'s study monitoring rCBV values greater than 1.5 to be indicative for high-grade gliomas and homogenously low rCBV less than 1.5 to be seen in most histologically proven low-grade gliomas (30).

Law et al. study reported in a study performed on 160 patients with cerebral gliomas, that rCBV cut-off ratio of 1.75 was a sensitive, but not specific, marker for high-grade histopathology, as all high-grade tumours had rCBV values greater than 1.75. No tumour with rCBV less than 1.75 was high-grade glioma (100% predictive value for excluding high grade) (18).

However, increased tumour vascularity can also be found in LGG, which will result in an elevated rCBV ratio. The pilocytic astrocytoma (WHO grade I), although biologically benign, has been described to exhibit histological evidence of angiogenesis and elevated rCBV ratio (31).

The low-grade oligodendrogliomas have also been reported to show elevated rCBV ratio due to their inherent dense network of branching capillaries resembling a ‘‘chicken wire ‘‘pattern. Xu et al. found no significant difference in rCBV ratio between low- and high-grade oligo- dendrogliomas (32).

Lev et al. reported that 50% of low-grade oligodendrogliomas presented elevated rCBV ratio (29).

Our study agrees with the studies by Lev et al. and Covarrubias et al. in rCBV ratio role for glioma grading but differs in cut-off values. For low-grade gliomas, they were ranging from 0.45 to 1.2 with mean value of rCBV 0.79 and rCBV ratio for high-grade gliomas ranging from 1.6 to 4.2 with mean value 2.62 & there was no HGG rCBV ratio less than 1.6 which agrees with Covarrubias et al. study.

The difference in values of cut-off between our study and the studies by Lev et al. and Covarrubias et al. was due to larger sample size & involving cases of LGG with high rCBV ratio that were not faced in our study.

In our study, rCBV were with high sensitivity & specificity reaching 100% for each in differentiation between HGG & LGG with cut-off value >1.2. rCBV cut-off value of (1.2) was considered as a sensitive & specific marker to predict high-grade gliomas as none of the examined low-grade gliomas showed rCBV higher than cut-off.

Though our study shows a good role for discrimination, the drawback in our study was a small sample size. We need further research & evaluation with a larger sample size & to do Meta analysis to be clinically applicable in the future. Regarding DTI (FA values), during determination of ROI to measure FA values, we should take in our consideration the values in contralateral area to calculate a corrected value as a ratio rather than a value. Also Computer-aided voxel-based semi-automated segmentation techniques may reduce the subjective bias inherent in manual ROI placement.

From the data obtained from our study, we can conclude that perfusion imaging is valuable in grading of cerebral gliomas by using the rCBV to give important information about the underlying neovascularity of the tumour regardless of the enhancement pattern of the lesion which agrees with Law et al., 2004 study (17).

The use of MR DTI had an important role in the grading of brain gliomas as it was accurate in grading 24 cases of gliomas (sensitivity of 100% and accuracy 100%).

Conflict of interest

The authors declare that there are no conflict of interests.

References

(1) Bruzzone MG, D'Incerti L, Farina LL, Cuccarini V, Finocchiaro GQ. J Nucl Med Mol Imag 2012;56(2):112–37.

(2) Brodbelt A. Clinical applications of imaging biomarkers. Part 2. The neurosurgeon's perspective. Br J Radiol 84 Spec No 2: S205–S208; 2011. http://dx.doi.org/10.1259/bjr/19282704.

(3) Roberts HC, Dillon WP. MR imaging of brain tumors: toward physiologic imaging. AJNR Am J Neuroradiol 2000;21 (9):1570–1.

(4) Hartmann M, Jansen O, Heiland S, Sommer C, Munkel K, Sartor K. Restricted diffusion within ring enhancement is not pathognomonic for brain abscess. AJNR Am J Neuroradiol 2001;22 (9):1738–42.

(5) Rizzo L, Crasto SG, Moruno PG, Cassoni P, Ruda R, Boccaletti R, et al. Role of diffusion- and perfusion-weighted MR imaging for brain tumour characterisation. Radiol Med 2009;114(4): 645–59.

(6) Hadziahmetovic M, Shirai K, Chakravarti A. Recent advancements in multimodality treatment of gliomas. Future Oncol 2011;7:1169–83.

(7) Stupp R, Tonn JC, Brada M, Pentheroudakis G. High-grade malignant glioma: ESMO Clinical Practice Guidelines for diagnosis, treatment and follow-up. Ann Oncol 2010;21:v190–3.

(8) Pouratian N, Schiff D. Management of low-grade glioma. Curr Neurol Neurosci Rep 2010;10:224–31.

(9) Lev MH, Ozsunar Y, Henson JW, et al. Glial tumor grading and outcome prediction using dynamic spin-echo MR susceptibility mapping compared with conventional contrast-enhanced MR: confounding effect of elevated rCBV of oligodendrogliomas. AJNR Am J Neuroradiol 2004;25:214–21 [PubMed].

(10) Law M, Oh S, Babb JS, et al. Low-grade gliomas: dynamic susceptibility-weighted contrast-enhanced perfusion MR imaging—prediction of patient clinical response. Radiology 2006;238: 658–67.

(11) Law M, Yang S, Wang H, et al. Glioma grading: sensitivity, specificity, and predictive values of perfusion MR imaging and proton MR spectroscopic imaging compared with conventional MR imaging. AJNR Am J Neuroradiol 2003;24:1989–98.

(12) Law M, Young RJ, Babb JS, et al. Gliomas: predicting time to progression or survival with cerebral blood volume measurements at dynamic susceptibility-weighted contrast-enhanced perfusion MR imaging. Radiology 2008;247:490–8.

(13) Cha S, Knopp EA, Johnson G, Wetzel SG, Litt AW, Zagzag D. Intracranial mass lesions: Dynamic contrast-enhanced susceptibility-weighted echo-planar perfusion MR imaging. Radiology 2002;223(1):11–29.

(14) Lee EJ, Ahn KJ, Lee EK, Lee YS, Kim DB. Potential role of advanced MRI techniques for the peritumoural region in differentiating glioblastoma multiforme and solitary metastatic lesions. Clin Radiol 2013;68:e689–97.

(15) Sanghvi DA. Recent advances in imaging of brain tumors. Indian J Cancer 2009;46(2):82–7.

(16) Law M, Oh S, Babb JS, et al. Low-grade gliomas: dynamic susceptibility-weighted contrast-enhanced perfusion MR imaging prediction of patient clinical response. Radiology 2006;238: 658–67.

(17) Law M, Yang S, Babb JS, Knopp EA, Golfinos JG, Zagzag D, et al. Comparison of cerebral blood volume and vascular permeability from dynamic susceptibility contrast-enhanced perfusion MR imaging with glioma grade. AJNR Am J Neuroradiol 2004;25(5):746–55.

(18) Law M, Yang S, Wang H, Babb JS, Johnson G, Cha S, et al. Glioma grading: sensitivity, specificity, and predictive values of perfusion MR imaging and proton MR spectroscopic imaging compared with conventional MR imaging. AJNR Am J Neuroradiol 2003;24(10):1989–98.

(19) Ginsberg LE, Fuller GN, Hashmi M, Leeds NE, Schomer DF. The significance of lack of MR contrast enhancement of supratentorial brain tumors in adults: histopathological evaluation of a series. Surg Neurol 1998;49(4):436–40.

(20) Lee EJ, Lee SK, Agid R, Bae JM, Keller A, Terbrugge K. Preoperative grading of presumptive low-grade astrocytomas on MR imaging: diagnostic value of minimum apparent diffusion coefficient. AJNRAm J Neuroradiol 2008;29:1872–7.

(21) Beppu T, Inoue T, Shibata Y, et al. Fractional anisotropy value by diffusion tensor magnetic resonance imaging as a predictor of cell density and proliferation activity of glioblastomas. Surg Neurol 2005;63:56–61.
(22) Inoue T, Ogasawara K, Beppu T, Ogawa A, Kabasawa H. Diffusion tensor imaging for preoperative evaluation of tumor grade in gliomas. Clin Neurol Neurosurg 2005;107:174–80.
(23) Kinoshita M, Hashimoto N, Goto T, et al. Fractional anisotropy and tumor cell density of the tumor core show positive correlation in diffusion tensor magnetic resonance imaging of malignant brain tumors. Neuroimage 2008;43:29–35.
(24) Misaki T, Beppu T, Inoue T, Ogasawara K, Ogawa A, Kabasawa H. Use of fractional anisotropy value by diffusion tensor MRI for preoperative diagnosis of astrocytic tumors: Case report. J Neurooncol 2004;70:343–8.
(25) Wang S, Kim S, Chawla S, et al. Differentiation between glioblastomas and solitary brain metastases using diffusion tensor imaging. Neuroimage 2009;44:653–60.
(26) Toh CH, Castillo M, Wong AM, et al. Differentiation between classic and atypical meningiomas with use of diffusion tensor imaging. AJNR Am J Neuroradiol 2008;29:1630–5.
(27) Senturk S, Oguz KK, Cila A. Dynamic contrast-enhanced susceptibility-weighted perfusion imaging of intracranial tumors: a study using a 3T MR scanner. Diagn Interv Radiol 2009;15 (1):3–12.
(28) Wong JC, Provenzale JM, Petrella JR. Perfusion MR imaging of brain neoplasms. AJR Am J Roentgenol 2000;174(4):1147–57.
(29) Lev MH, Ozsunar Y, Henson JW, Rasheed AA, Barest GD, Harsh GRt, et al. Glial tumor grading and outcome prediction using dynamic spin-echo MR susceptibility mapping compared with conventional contrast-enhanced MR: confounding effect of elevated rCBV of oligodendrogliomas [corrected]. AJNR Am J Neuroradiol 2004;25(2):214–21.
(30) Covarrubias DJ, Rosen BR, Lev MH. Dynamic magnetic resonance perfusion imaging of brain tumors. Oncologist 2004;9 (5):528–37.
(31) Shin JH, Lee HK, Kwun BD, Kim JS, Kang W, Choi CG, et al. Using relative cerebral blood flow and volume to evaluate the histopathologic grade of cerebral gliomas: preliminary results. AJR Am JRoentgenol 2002;179(3):783–9.
(32) Cha S, Tihan T, Crawford F, et al. Differentiation of low-grade oligodendrogliomas from low-grade astrocytomas by using quantitative blood volume measurements derived from dynamic susceptibility contrast-enhanced MR imaging. AJNR Am J Neuroradiol 2005;26:266–73.